

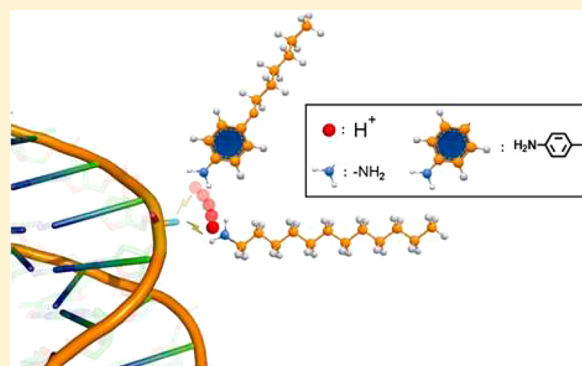
High-Density Noncovalent Functionalization of DNA by Electrostatic Interactions

Wei Chen, Jennifer Y. Gerasimov, Pei Zhao, Kai Liu, and Andreas Herrmann*

Zernike Institute for Advanced Materials, Department of Polymer Chemistry, University of Groningen, Nijenborgh 4, 9747 AG Groningen, Netherlands

S Supporting Information

ABSTRACT: Preserving DNA hybridization in organic solvents could someday serve to significantly extend the applicability of DNA-based technologies. Here, we present a method that can be used to solubilize double-stranded DNA at high concentrations in organic media. This method requires first precipitating a DNA molecule from the aqueous environment with an anilinium derivative and subsequently exchanging this moiety with an amine-containing surfactant in organic solvent. We demonstrate that this method yields complete exchange of the surfactant and allows for the modification of DNA with hydrophobic primary, secondary, and tertiary alkylamines and ordered functional π -systems. Using this approach, we fabricate a multichromophoric light harvesting system that would be unattainable by traditional methods. Additionally, this method makes it possible to use small, hydrophilic molecules to solubilize DNA in organic solvents, which reduces the shielding around the DNA and makes the macromolecule more accessible for further chemical modification. We believe that this approach will prove tremendously beneficial in expanding the scope of DNA-based nano- and biotechnologies.



INTRODUCTION

Aside from its role as the universal carrier of genetic information, DNA has found widespread application in directing the bottom-up fabrication of nanoobjects and hybrid assemblies. Due to its rigid structure and its programmable self-recognition properties,¹ double-helical DNA may be implemented as a structural scaffold, or template, to organize materials in one, two, and three dimensions.^{2,3} DNA-mediated scaffolding thus provides the means to exercise spatial control over reactions and catalytic processes at the nanometer scale.^{2a-c,3b} Furthermore, DNA templates integrate seamlessly into existing DNA technologies, among them, sensors,⁴ photonic wires,⁵ and light-harvesting systems.⁶

While most DNA technologies are developed for use in aqueous environments, the demonstration that cationic lipids can solubilize DNA in organic solvents has triggered growing interest in employing DNA in nonaqueous systems.⁷ Solubilization in nonpolar organic solvents is possible because cationic head groups electrostatically interact with phosphate groups to displace the charged metal cations. Subsequently, lipophilic tail groups induce cooperative hydrophobic interactions, promoting the aggregation of DNA and the entropically driven release of salt.⁸ As a result, the DNA–lipid complex precipitates out of the aqueous solution, but can be easily dissolved in many organic solvents. In the organic phase, DNA–lipid complexes have been used to study mechanical^{7,9} and conductivity properties of DNA.¹⁰ Apart from these

fundamental investigations, DNA–surfactant complexes have also been utilized to manipulate the mesophase behavior of liquid crystals,^{8b,c,11} to act as an integral element for electronics,¹² to serve as a scaffold for biomineralization,¹³ to fabricate organogels,¹⁴ and as a vehicle for gene delivery.¹⁵

Unfortunately, the broader integration of these materials into functional systems and devices is limited by the solubility of the surfactant used. As it stands, the solubilizing surfactant is constrained to having linear alkyl chains with lengths ranging from 8 to 16 carbons.⁸ To enable exchange of the metal counterion on the DNA backbone with a cationic surfactant, the lipid moiety needs to be sufficiently hydrophilic to be introduced into the aqueous phase, but hydrophobic enough to cause DNA aggregation.⁸ Very few cationic amphiphiles currently meet these requirements, which imposes rather rigid constraints on the innovation of nonaqueous DNA technologies.¹²

In this contribution, we present a novel method that overcomes solubility limitations and allows the electrostatically driven decoration of DNA with a much wider range of functionalities. To introduce DNA-complexing molecules that exhibit poor solubility in water, we developed a two-step method that relies on a water-soluble surfactant to solubilize the DNA in the organic phase, where it can subsequently be

Received: May 26, 2015

Published: September 24, 2015

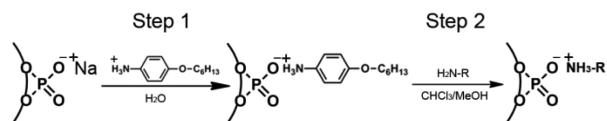
exchanged for a more hydrophobic amine-containing surfactant. We found, however, that simple substitution of surfactants is rather problematic due to the infrequent dissociation of ion pairs in the organic phase. We therefore introduced an energetically favorable proton transfer to accompany the surfactant exchange, which drives the reaction to completion. This strategy is the first reported approach to functionalizing DNA in the organic phase by ligand exchange. We demonstrate that this approach is compatible with a broad range of hydrophobic surfactants, including long chain hydrocarbons and conjugated π -systems as well as hydrophilic alkylamines that would not otherwise induce the precipitation of DNA in aqueous solutions.

RESULTS AND DISCUSSION

DNA Precipitation. To solubilize DNA in an organic solvent, we introduce 4-(hexyloxy)anilinium (ANI) into an aqueous solution of double-stranded DNA (dsDNA, 2000 base pairs). As the cationic ANI headgroup electrostatically interacts with the anionic phosphodiester backbone, a hydrophobic hydrocarbon shell envelops the dsDNA molecules.¹⁶ As a result, the DNA–ANI complex precipitates out of solution and is collected by centrifugation.

ANI Substitution with Saturated Aliphatic Surfactants. As a proof of principle experiment, we investigate the substitution of DNA-complexed ANI with dodecylamine—a surfactant that is insoluble in water and thus a poor candidate for traditional methods of DNA modification by cationic surfactants (Scheme 1). The substitution was carried out in a

Scheme 1. Two-Step Process for the Formation of a DNA–Surfactant Complex with Amine Surfactants



mixture of methanol and chloroform (4:1 $\text{CHCl}_3/\text{MeOH}$), using a 3-fold excess of amine-containing surfactant in relation to the negative charges of the DNA. The final concentration of DNA is $1 \mu\text{M}$, and that of the surfactant is 12 mM . After mixing and stirring for about 5 min, the solution was transferred into regenerated cellulose dialysis tubing (molecular weight cutoff, 10,000 Da) and dialyzed against $\text{CHCl}_3/\text{MeOH}$ to remove excess dodecylamine and ANI.

After purification through dialysis, the ^1H NMR spectra of dodecylammonium (DA) chloride and pristine dodecylamine were compared to the spectrum of the DNA–DA complex (Figure 1). The peak of the α -methylene group in the spectrum of the DNA–surfactant complex (2.72 ppm) appears in a position similar to the uncomplexed DA (2.76 ppm), but is shifted downfield by 0.2 ppm in comparison to the free dodecylamine. We interpret this as evidence that the DNA-encapsulating surfactant is present in the charged state. In the spectrum of the protonated DA, the α -methylene peak is well-resolved as a triplet, whereas the peak appears broad and unresolved upon interrogation of the DNA–surfactant complex. The broadening of the signal can be explained by the restricted mobility of the surfactant when it is localized around DNA. Alternatively, the broad signal could indicate the aggregation of the DNA–lipid complex. To exclude the possibility of aggregation, we examined the dynamic light

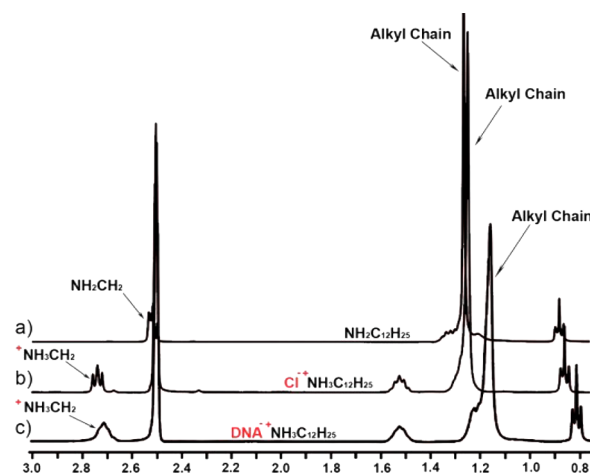


Figure 1. ^1H NMR spectrum of the DNA–DA complex ($\text{DNA}^-\text{NH}_3\text{C}_{12}\text{H}_{25}$), DA ($\text{Cl}^+\text{NH}_3\text{C}_{12}\text{H}_{25}$), and dodecylamine ($\text{NH}_2\text{C}_{12}\text{H}_{25}$) in d-DMSO.

scattering behavior of a long-chain dodecylammonium lipid–DNA complex in 4:1 $\text{CHCl}_3/\text{MeOH}$ and a short-chain triethylammonium–DNA complex in MeOH. To avoid unspecific structure formation, we used a short nonself-complementary synthetic DNA oligomer (22mer), synthesized in-house to prepare the above complex. The DNA concentration was found by UV absorption to be $75 \mu\text{M}$ for the long-chain complex and $100 \mu\text{M}$ for the short-chain complex. The raw correlation data show no correlation between the intensity autocorrelation function and the lag time, which demonstrates that neither the DNA–dodecylammonium (Figure S1) nor the DNA–triethylammonium (Figure S2) complex form aggregates at high concentrations (75 – $100 \mu\text{M}$). Further, the broadened NMR signature is only apparent for the proton near the DNA strand while the proton at the end of the ligand chain (0.8 ppm) does not exhibit this phenomenon. It is therefore reasonable to deduce the restricted mobility rather than aggregation causes a decrease in resolution of the triplet from the amine group; otherwise, every proton signal should exhibit peak broadening in the NMR spectrum. The signal at 1.15 ppm, assigned to the other methylene groups in DNA–DA, appears at higher field in relation to uncomplexed DA. This behavior can be attributed to a difference in the environment surrounding the alkyl chains when they are complexed to the DNA in a brush-like structure, where neighboring chains are in contact with each other, as opposed to the free state, where the alkyl chains are surrounded by solvent. Additionally, the peaks at 6.69 ppm, which belong to the benzene ring of ANI, are absent in the spectrum of the DNA–surfactant complex (Figure S3). This set of NMR experiments demonstrates that the ANI moieties were completely replaced by DA. Unexpectedly, no proton signals originating from the DNA were detected in the spectrum of the complex, indicating a high propensity of DA to screen DNA proton resonances.

Optical methods were used to further characterize the DNA–DA complex. The ultraviolet–visible (UV/vis) spectrum of the complex exhibits the distinctive DNA absorbance maximum at 260 nm, indicating that DNA is indeed dissolved in $\text{CHCl}_3/\text{MeOH}$ (Figure 2). Circular dichroism (CD) spectroscopy provides structural information about the DNA–DA complex in organic media. Positive and negative CD signals at 289 and 258 nm, respectively, are indicative of

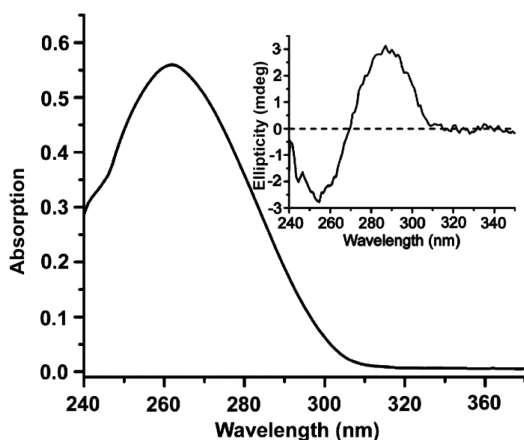


Figure 2. UV-vis and CD (inset) spectra of the DNA-DA complex. DNA concentration is $0.02 \mu\text{M}$ in 4:1 $\text{CHCl}_3/\text{MeOH}$.

the right-handed double helix structure of DNA (Figure 2, inset). As previously observed upon complexation with cationic surfactants, CD peaks shift to longer wavelengths and decrease in intensity compared to double stranded DNA in aqueous solvent. This has previously been attributed to a transition from the B-form of DNA, found under physiological conditions, to the C-form.^{17a} More recent studies, however, have concluded that the changes in the CD signal are a result of minor changes in the interactions between the bases and that the double helix maintains the B-form.^{17b,c} The transition could be the result of the absence of water molecules around DNA that interact with the oxygen of ribose, phosphate, and minor or major grooves.^{7a,17}

Finally, the successful exchange of the cationic surfactant was verified by Fourier Transform Infrared (FTIR) spectroscopy. It can be seen from the IR spectrum (Figure S2) that the DNA-DA complex shows characteristic ammonium bands that absorb in a range between 3191 and 3142 cm^{-1} and at 1650 cm^{-1} , corresponding to N-H stretching and asymmetrical $-\text{NH}_3^+$ deformation vibrations, respectively.¹⁸ The IR-bands at 1058 and 1238 cm^{-1} are assigned to symmetric and asymmetric stretching vibrations of PO_2^- groups of DNA.¹⁹

Other alkyl amines that cannot be attached to DNA in a direct, single-step procedure, including octadecylamine, dioctadecylamine, and trioctylamine, were also shown to be compatible with this two-step method of ligand exchange. For characterization, please see Supporting Information (Figures S5–S10). This approach also works well with a longer synthetic duplex. We chose two complementary nucleotides (48mer), oligo 1 and oligo 2, used in DNA origami, to demonstrate the feasibility. The sequences can be found in the Supporting Information. Both the hybridized duplex and single-stranded oligonucleotides (oligo 1 and 2) were first precipitated by ANI in the aqueous phase and subsequently extracted into a mixture of methanol and chloroform (4:1 $\text{CHCl}_3/\text{MeOH}$), where ANI was substituted by dodecylamine. The final concentrations of the duplex and single-stranded oligomers were adjusted to $1.2 \mu\text{M}$ by monitoring the UV absorption at 260 nm . CD data (Figure S11) of oligo 1 in the DNA region exhibit a broad positive ellipticity peak with a maximum at 270 nm . The maximum negative ellipticity is difficult to identify due to the high noise from organic solvent below 245 nm . Oligo 2 shows both positive and negative ellipticity at 284 and 255 nm , respectively. The duplex shows a similar profile to Oligo2, with

positive and negative ellipticity at 284 and 247 nm , but with higher CD intensity of both positive and negative peaks due to the formation of the double-stranded helical structure.

ANI Substitution with Conjugated Polycyclic Surfactant. DNA has proven to be a very promising template to spatially control the arrangement of photoactive materials on the nanoscale²⁰ and has been used for the fabrication of luminescent thin films via precise arrangement of fluorescent donors and acceptors.²¹ Here, we synthesize a terthiophene conjugate with an amine headgroup, designed to form a supramolecular assembly of functional π -conjugated systems around a DNA double helix (Figure 3a). The synthesis and

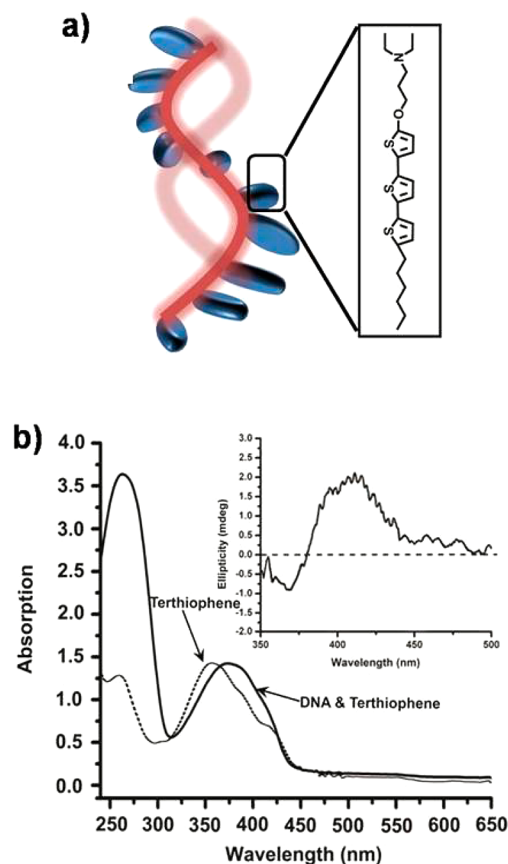


Figure 3. Molecular structure of terthiophene modified with an amine group for complexation with DNA (a). UV-vis absorption spectra of films of terthiophene and the DNA-terthiophene complex prepared from $0.5 \mu\text{M}$ DNA complex solution (b). Inset: CD spectrum of the DNA-terthiophene complex.

characterization of this compound are detailed in the Supporting Information. Terthiophene is soluble in most organic solvents and can therefore be introduced to encapsulate DNA according to the procedure described above. After thorough purification of the DNA-terthiophene complex in the organic phase (4:1 $\text{CHCl}_3/\text{MeOH}$), which resulted in a solution containing $0.5 \mu\text{M}$ DNA complex, thin films were cast and examined by UV-vis and CD spectroscopy.

The UV-vis absorption spectra of pristine terthiophene and the DNA-terthiophene complex differ markedly from each other. In the spectrum of DNA-terthiophene a much larger absorption peak is detected at a wavelength of 260 nm in relation to the pristine terthiophene moiety, which can be attributed to the presence of the nucleic acid component. The

maximum absorption of terthiophene is located at 356 nm while the corresponding maximum of the DNA–terthiophene complex is found at 374 nm, exhibiting an 18 nm bathochromic shift. This spectral behavior is indicative of the formation of J-aggregates of the aromatic oligothiophene system.^{4c}

CD data in the spectral region of terthiophene absorption exhibit positive ellipticity with a peak maximum at 415 nm and weak negative ellipticity at 369 nm, with zero-crossing at 378 nm (Figure 3b, inset). In contrast, for bare terthiophene films, no CD signal is measured. The CD data suggest that the terthiophene molecules are assembled in a right-handed helix as a result of being complexed with the DNA molecule.²² These experiments demonstrate that through the application of our new surfactant exchange strategy, it is possible to organize functional molecules in a way that enables the production of supramolecular π -system architectures that employ DNA as a template. Due to the hydrophobic character of extended aromatic units, such chromophore ensembles are not attainable via existing methods for formation of DNA–surfactant complexes.

ANI Substitution with Pyrene To Mimic Light Harvesting Systems. Having demonstrated ligand exchange with an aromatic surfactant, we further explore this strategy to construct a noncovalent light harvesting system (LHS). Such complexes play a key role in photosynthesis by funneling electronic excitations, which are induced by sunlight, toward the reaction center by energy transfer.²³ Due to the importance of this process, several model LHSs have been synthesized.²⁴ To fabricate a DNA–surfactant complex that mimics an LHS, a 22mer oligonucleotide was labeled at one terminus with a chromophore that exhibits a large Stokes shift (490LS, ATTO-TEC). This chromophore is characterized by an optical absorption ranging from 450 to 550 nm (absorption maximum 496 nm) and an emission maximum at 620 nm. Using the novel surfactant exchange method described in the previous sections, the 490LS-labeled oligonucleotide is complexed with a pyrene-modified surfactant (Figure 4a). The synthesis and characterization of this compound are detailed in the Supporting Information. The UV/vis absorption of DNA–490LS pyrene complex (black curve) is shown in Figure 4b, which exhibits the characteristic maximum absorption of pyrene (250 to 280, and 300 to 355 nm) and that of DNA (260 nm). The weak absorption peak at 496 nm can be assigned to 490LS. As a control, we examine the emission spectrum of a DNA–pyrene surfactant complex that is not labeled with 490LS. Both DNA–490LS–pyrene (red curve) and DNA–pyrene (blue curve) exhibit a broad emission peak between 420 and 500 nm, with a maximum at 450 nm (Figure 4b). These bands are ascribed to excimer fluorescence that is caused by the aggregation of pyrene along the DNA scaffold.²⁵ Due to the overlap of pyrene emission and 490LS absorption, in addition to the close proximity of both types of chromophores within the DNA–surfactant complex, energy transfer is observed as 490LS emission at 610 nm. Comparing the LHS with the control, the spectrum of the DNA–490LS–pyrene complex exhibits lower pyrene photoluminescence in relation to the DNA–pyrene complex, indicating that the energy is transferred to the acceptor. In a separate experiment, we determined that when pyrene is introduced, but not complexed with 490LS-labeled DNA, no energy transfer is observed. These photophysical measurements prove that a simple surfactant exchange method can enable the successful construction of a functioning LHS.

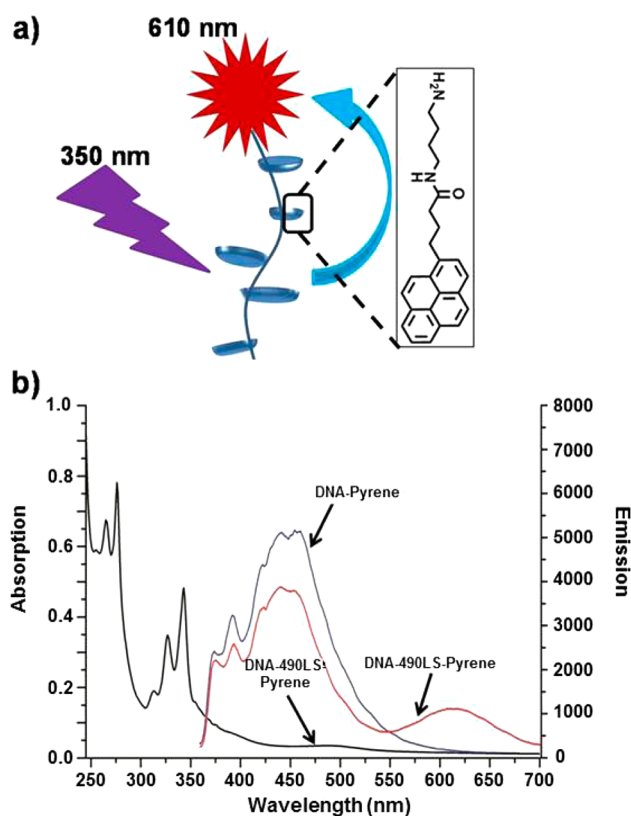


Figure 4. (a) Illustration of energy transfer from DNA bonded pyrene to 490LS in the LHS. (b) UV/vis absorption (black) and emission (red) of DNA–490LS–pyrene complex. The emission of a DNA–pyrene complex in organic solvent (4:1 $\text{CHCl}_3/\text{MeOH}$) with concentration 0.4 μM , absent 490LS is presented as a control (blue). The excitation wavelength for all emission spectra is 350 nm.

ANI Substitution with Water-Soluble Surfactants.

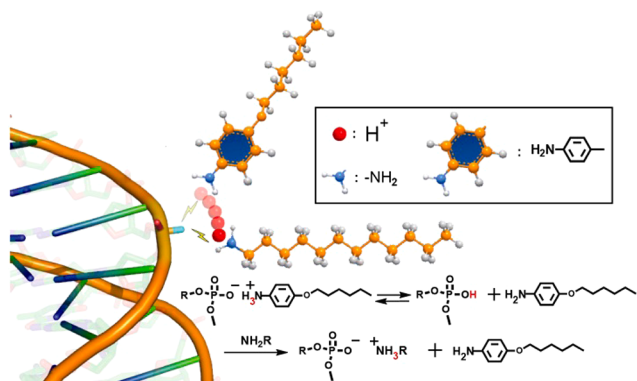
Reducing the steric hindrance of the surfactant shell around the DNA could potentially have a significant impact on the effectiveness of noncovalent DNA functionalization²⁶ and DNA-mediated catalysis in the organic phase.²⁷ DNA solubilization by small ligands in organic solvents presents a different set of challenges. Small amine ligands are more hydrophilic compared to larger surfactant molecules and thus do not evoke DNA precipitation in aqueous environments, making the complex more difficult to isolate.²⁸ Since the two-step exchange protocol does not rely on coprecipitation of DNA with the selected surfactant in an aqueous solvent, we can investigate the lower size limits of small ligands that keep DNA soluble in the organic phase. While amines with a lower molecular weight, such as diethylammonium and dimethylammonium, precipitate in most organic solvents, we found that triethylammonium can be used to replace ANI in the organic phase and solubilize DNA from salmon testes (2000 bp) in $\text{CHCl}_3/\text{MeOH}$ (for characterization, see Supporting Information Figures S12 and S13). Because significantly smaller cationic ligands are used here than in the previous sections, the proton signals from the nucleobase and the pentose are clearly visible in the NMR spectrum of the DNA–triethylammonium complex (Figure S9). The peaks at 4.74 ppm ($\text{H}3'$), 4.14 ppm ($\text{H}4'$), 3.88 ppm ($\text{H}5'$, $\text{H}5''$), and 1.78 ppm ($\text{H}2'$) are attributed to protons on the pentose. By integrating the ^1H NMR signals, we determine that the molecular ratio of pentose to triethylammonium is close to 1:1.

This is yet another strong indicator that one phosphate group is complexed with one cationic ligand and that the ligand exchange proceeds to completion. Although short, unmodified DNA strands (10–30 bp) have previously been introduced into tetrahydrofuran and acetonitrile for DNA-templated reactions, their concentration has been limited to the nanomolar range.²⁶ In contrast, here, micromolar DNA concentrations were reached in organic solvents with the small counterion triethylammonium.

Exchange Mechanism. According to models developed to describe ion-exchange chromatographic separations, the rate of ion exchange depends on the charge of a given ion and its mobility in the selected solvent.²⁹ Both of these parameters determine the degree of ion pair dissociation and are controlled by electrostatic interactions. According to Coulomb's law,³⁰ the force between counterions is inversely proportional to the dielectric constant of the solvent. To achieve effective substitution of an ion pair, the exchange process should be carried out in a solvent with a high dielectric constant ($\epsilon\gamma$), such as water ($\epsilon\gamma \approx 80.1$), or water mixtures containing polar solvents, such as acetonitrile ($\epsilon\gamma \approx 37.5$). In contrast, we achieved ligand exchange in a nonpolar environment containing chloroform ($\epsilon\gamma \approx 4.8$), where cation mobility is significantly lower. The effective, high-yield exchange of the surfactant in a nonpolar solvent suggests that a chemical process contributes to the exchange in addition to the purely physical diffusion mechanism.

We propose the following mechanism to accommodate our observations. The DNA–ANI interaction can be characterized as an ionic hydrogen bond between the phosphate of the DNA backbone and the ammonium group of the ANI. As such, both electrostatic and acid–base interactions contribute to the stability of the bond.³¹ With the introduction of a primary amine, the acid–base interaction is disrupted because aniline has a much lower K_b value ($\sim 10^{-10}$ M) than the primary amine ($\sim 10^{-4}$ M). Therefore, amines exhibit a much higher reactivity with phosphoric acid than the aniline group. We postulate that the substitution of the ANI for the primary amine is the result of a proton transfer between the two surfactants participating in the exchange (Scheme 2). This transfer is facilitated by the phosphate anion, which is transiently protonated and can therefore react with the amine group of the more basic surfactant. After the transfer, the phosphate anion electrostatically interacts with the cationic ammonium group. This leaves the now-neutral aniline free to dissociate from the DNA–

Scheme 2. Schematic Representation of the Mechanism of Exchanging the ANI Component with a Primary Amine



ammonium complex. In accordance with our theory, the rate of substitution is determined by the differences in K_b values between the primary amine and aniline. Since the basicity of primary, secondary, and tertiary amines is orders of magnitude larger than that of aniline, there is sufficient driving force to ensure complete cation exchange, as observed in our experiments.

CONCLUSION

We have developed a robust and generic protocol for the noncovalent modification of single-stranded and double-stranded DNA by ligand exchange in organic solvents. The method requires first precipitating a DNA molecule with an anilinium compound from the aqueous environment and subsequently exchanging this moiety with an amine in an organic solvent. This strategy provides an alternative way to fabricate DNA–lipid complexes, overcoming the very restricted window of surfactant solubility required for the direct exchange mechanism. Due to the large driving force of proton exchange between the anilinium and the amine, the exchange process runs to completion, as proven by NMR studies.

Therefore, the DNA–surfactant systems reported herein differ significantly from the ones reported earlier,^{7–16} where the choice of surfactants was limited to a great extent. Moreover, the electrostatic complexes depart from previous work where the complexation of the DNA with the surfactant enabled overcoming solubility incompatibilities to modify hydrophilic nucleic acid moieties with hydrophobic units through covalent bond formation.^{8d} This novel noncovalent method of functionalization allows the fabrication of DNA ensembles in the organic phase where the double helix is surrounded by primary, secondary, and tertiary hydrophobic alkylamines, ordered functional π -systems, and even small hydrophilic molecules. Finally, we demonstrate the successful construction of a multichromophoric light harvesting system based on DNA–surfactant complexes. We believe that this approach may greatly accelerate the fabrication of functional DNA nanostructures.

ASSOCIATED CONTENT

Supporting Information

The Supporting Information is available free of charge on the ACS Publications website at DOI: 10.1021/jacs.5b05432.

Detailed description of the methods, materials, synthesis of ANI, synthesis of *N,N*-diethyl-3-((5''-hexyl-[2,2':5',2''-terthiophen]-5-yl)oxy)propan-1-amine, synthesis of pyrene, ¹H NMR of DNA–ANI complex, Fourier transform infrared spectra of DNA–lipid complexes, characterization of DNA–octadecylammonium, –dioctadecylammonium, –trioctylammonium, and –triethylammonium complexes (PDF)

AUTHOR INFORMATION

Corresponding Author

*a.herrmann@rug.nl

Notes

The authors declare no competing financial interest.

ACKNOWLEDGMENTS

W.C. and A.H. were supported by the EU (ERC starting grant and STREP project Microagents), The Netherlands Organization for Scientific Research (NWO-Vici), and the Zernike

Institute for Advanced Materials. Discussions with Lifei Zheng are gratefully acknowledged.

REFERENCES

- (1) (a) Seeman, N. C. *Annu. Rev. Biochem.* **2010**, *79*, 65. (b) Stulz, E.; Clever, G.; Shionoya, M.; Mao, C. *Chem. Soc. Rev.* **2011**, *40*, 5633. (c) Han, D.; Pal, S.; Yang, Y.; Jiang, S.; Nangreave, J.; Liu, Y.; Yan, H. *Science* **2013**, *339*, 1412. (d) Kwak, M.; Minten, I. J.; Anaya, D. M.; Musser, A. J.; Brasch, M.; Nolte, R. J. M.; Müllen, K.; Cornelissen, J. L. M.; Herrmann, A. *J. Am. Chem. Soc.* **2010**, *132*, 7834.
- (2) (a) Chen, W.; Schuster, G. B. *J. Am. Chem. Soc.* **2012**, *134*, 840. (b) Ma, Y.; Zhang, J.; Zhang, G.; He, H. *J. Am. Chem. Soc.* **2004**, *126*, 7097. (c) Chen, W.; Schuster, G. B. *J. Am. Chem. Soc.* **2013**, *135*, 4438. (d) Li, X.; Liu, D. R. *Angew. Chem., Int. Ed.* **2004**, *43*, 4848. (e) Kleiner, R. E.; Dumelin, C. E.; Liu, D. R. *Chem. Soc. Rev.* **2011**, *40*, 5707.
- (3) (a) Boersma, A. J.; Megens, R. P.; Feringa, B. L.; Roelfes, G. *Chem. Soc. Rev.* **2010**, *39*, 2083. (b) Prusty, D. K.; Kwak, M.; Wildeman, J.; Herrmann, A. *Angew. Chem., Int. Ed.* **2012**, *51*, 11894.
- (4) (a) Huang, J.; Wu, Y.; Chen, Y.; Zhu, Z.; Yang, X.; Yang, C. D.; Wang, K.; Tan, W. *Angew. Chem., Int. Ed.* **2011**, *50*, 401. (b) Prusty, D. K.; Herrmann, A. *J. Am. Chem. Soc.* **2010**, *132*, 12197. (c) Ergen, E.; Weber, M.; Jacob, J.; Herrmann, A.; Müllen, K. *Chem. - Eur. J.* **2006**, *12*, 3707. (d) Marras, S. A. E.; Tyagi, S.; Kramer, F. R. *Clin. Chim. Acta* **2006**, *363*, 48. (e) Teo, Y. N.; Kool, E. T. *Chem. Rev.* **2012**, *112*, 4221.
- (5) (a) Heilemann, M.; Tinnefeld, P.; Mosteiro, G. S.; Parajo, M. G.; Van Hulst, N. F.; Sauer, M. *J. Am. Chem. Soc.* **2004**, *126*, 6514. (b) Heilemann, M.; Kasper, R.; Tinnefeld, P.; Sauer, M. *J. Am. Chem. Soc.* **2006**, *128*, 16864. (c) Kumar, C. V.; Duff, M. R. *J. Am. Chem. Soc.* **2009**, *131*, 16024. (d) Woller, J. G.; Hannestad, J. K.; Albinsson, B. *J. Am. Chem. Soc.* **2013**, *135*, 2759.
- (7) (a) Tanaka, K.; Okahata, Y. *J. Am. Chem. Soc.* **1996**, *118*, 10679. (b) Yang, C.; Moses, D.; Heeger, A. *Adv. Mater.* **2003**, *15*, 1364. (c) Neumann, T.; Gajria, S.; Bouxsein, N. F.; Jaeger, L.; Tirrell, M. *J. Am. Chem. Soc.* **2010**, *132*, 7025. (d) Wang, L.; Yoshida, J.; Ogata, N. *Chem. Mater.* **2001**, *13*, 1273. (e) Rosa, M.; Dias, R.; Miguel, M. G.; Lindman, B. *Biomacromolecules* **2005**, *6*, 2164. (f) Dias, R. S.; Magno, L. M.; Valente, A. J. M.; Das, D.; Das, P. K.; Maiti, S.; Miguel, M. G.; Lindman, B. *J. Phys. Chem. B* **2008**, *112*, 14446.
- (8) (a) Matulis, D.; Rouzina, L.; Bloomfield, V. A. *J. Am. Chem. Soc.* **2002**, *124*, 7331. (b) Liu, K.; Chen, D.; Marcozzi, A.; Zheng, L.; Su, J.; Pesce, D.; Zajaczkowski, W.; Kolbe, A.; Pisula, W.; Müllen, K.; Clark, N. A.; Herrmann, A. *Proc. Natl. Acad. Sci. U. S. A.* **2014**, *111*, 18596. (c) Liu, K.; Shuai, M.; Chen, D.; Tuchband, M.; Gerasimov, J. Y.; Su, J.; Liu, Q.; Zajaczkowski, W.; Pisula, W.; Müllen, K.; Clark, N. A.; Herrmann, A. *Chem. - Eur. J.* **2015**, *21*, 4898. (d) Liu, K.; Zheng, L.; Liu, Q.; de Vries, J. W.; Gerasimov, J. Y.; Herrmann, A. *J. Am. Chem. Soc.* **2014**, *136*, 14255.
- (9) Fukushima, T.; Hayakawa, T.; Inoue, Y.; Miyazaki, K.; Okahata, Y. *Biomaterials* **2004**, *25*, 5491.
- (10) (a) Okahata, Y.; Kobayashi, T.; Tanaka, K.; Shimomura, M. *J. Am. Chem. Soc.* **1998**, *120*, 6165. (b) Nishimura, N.; Nomura, Y.; Nakamura, N.; Ohno, H. *Biomaterials* **2005**, *26*, 5558.
- (11) Cui, L.; Zhu, L. *Langmuir* **2006**, *22*, 5982.
- (12) (a) Hagen, J. A.; Li, W.; Steckl, J.; Grote, J. G. *Appl. Phys. Lett.* **2006**, *88*, 171109. (b) Heckman, D. E. M.; Grote, J. G.; Hopkins, F. K.; Yaney, P. P. *Appl. Phys. Lett.* **2006**, *89*, 181116. (c) Wanapun, D.; Hall, V. J.; Begue, N. J.; Grote, J. G.; Simpson, G. J. *ChemPhysChem* **2009**, *10*, 2674.
- (13) Liang, H.; Angelini, T. E.; Ho, J.; Braun, P. V.; Wong, G. C. L. *J. Am. Chem. Soc.* **2003**, *125*, 11786.
- (14) (a) Numata, M.; Sugiyasu, K.; Kishida, T.; Haraguchi, S.; Fujita, N.; Park, S. M.; Yun, Y. J.; Kim, B. H.; Shinkai, S. *Org. Biomol. Chem.* **2008**, *6*, 712. (b) Sugiyasu, K.; Numata, M.; Fujita, N.; Park, S. M.; Yun, Y. J.; Kim, B. H.; Shinkai, S. *Chem. Commun.* **2004**, *17*, 1996.
- (15) Aytar, B. S.; Muller, J. P. E.; Kondo, Y.; Talmon, Y.; Abbott, N. L.; Lynn, D. M. *J. Am. Chem. Soc.* **2013**, *135*, 9111.
- (16) Uemura, S.; Shimakawa, T.; Kusabuka, K.; Nakahira, T.; Kobayashi, N. *J. Mater. Chem.* **2001**, *11*, 267.
- (17) (a) Prive, G. G.; Heinemann, U.; Chandrasegaran, S.; Kan, L. S.; Kopka, M. L.; Dickerson, R. E. *Science* **1987**, *238*, 498. (b) Braun, C. S.; Jas, G. S.; Choosakoonkriang, S.; Koe, G.; Smith, J. G.; Middaugh, C. R. *Biophys. J.* **2003**, *84*, 1114. (c) Middaugh, C. R.; Ramsey, J. D. *Anal. Chem.* **2007**, *79*, 7240.
- (18) Serratos, J. M.; Johns, W. D.; Shimoyama, A. *Clays Clay Miner.* **1970**, *18*, 107.
- (19) Ding, Y.; Zhang, L.; Xie, J.; Guo, R. *J. Phys. Chem. B* **2010**, *114*, 2033.
- (20) Su, W.; Bonnard, V.; Burley, G. *Chem. - Eur. J.* **2011**, *17*, 7982.
- (21) Ner, Y.; Grote, J. G.; Stuart, J. A.; Sotzing, G. A. *Angew. Chem., Int. Ed.* **2009**, *48*, 5134.
- (22) (a) Janssen, P. G. A.; Carretero, A. R.; Rodriguez, D. G.; Meijer, E. W.; Schenning, A. P. H. *J. Angew. Chem., Int. Ed.* **2009**, *48*, 8103. (b) Janssen, P. G. A.; Meeuwenoord, N.; Marel, G.; Farouji, S. J.; Schoot, P.; Surin, M.; Tomovic, Z.; Meijer, E. W.; Schenning, A. P. H. *J. Chem. Commun.* **2010**, *46*, 109.
- (23) Hu, X.; Damjanovic, A.; Ritz, T.; Schulten, K. *Proc. Natl. Acad. Sci. U. S. A.* **1998**, *95*, 5935.
- (24) Liu, D. J.; De Feyter, S.; Cotlet, M.; Stefan, A.; Wiesler, U. M.; Herrmann, A.; Grebel-Köhler, D.; Qu, J.; Müllen, K.; De Schryver, F. C. *Macromolecules* **2003**, *36*, 5918.
- (25) Nishizawa, S.; Kato, Y.; Teramae, N. *J. Am. Chem. Soc.* **1999**, *121*, 9463. Cuppoletti, A.; Cho, Y.; Park, J. S.; Strassler, C.; Kool, E. T. *Bioconjugate Chem.* **2005**, *16*, 528.
- (26) Rozenman, M. M.; Liu, D. R. *ChemBioChem* **2006**, *7*, 253.
- (27) Megens, R. P.; Roelfes, G. *Org. Biomol. Chem.* **2010**, *8*, 1387.
- (28) Abe, H.; Abe, N.; Shibata, A.; Ito, K.; Tanaka, Y.; Ito, M.; Saneyoshi, H.; Shuto, S.; Ito, Y. *Angew. Chem., Int. Ed.* **2012**, *51*, 6475.
- (29) Helfferich, F. *Ion Exchange*; Courier Dover Publications: 1962 print.
- (30) Amis, E. M. *J. Chem. Educ.* **1951**, *28*, 635.
- (31) Staib, A.; Borgis, D.; Hynes, J. T. *J. Chem. Phys.* **1995**, *102*, 2487.